

Received April 9, 2019, accepted May 1, 2019, date of publication May 8, 2019, date of current version July 2, 2019.

Digital Object Identifier 10.1109/ACCESS.2019.2915596

An Optimized Image Watermarking Method Based on HD and SVD in DWT Domain

JUNXIU LIU¹, (Member, IEEE), JIADONG HUANG¹, YULING LUO¹, LVCHEN CAO²,
SU YANG³, DUQU WEI¹, AND RONGLONG ZHOU¹

¹School of Electronic Engineering, Guangxi Normal University, Guilin 541004, China

²School of Information and Electronics, Beijing Institute of Technology, Beijing 100081, China

³School of Computing, Engineering and Intelligent Systems, Ulster University, Londonderry BT48 7JL, U.K.

Corresponding author: Yuling Luo (yuling0616@gxnu.edu.cn)

This work was supported in part by the National Natural Science Foundation of China under Grant 61801131, Grant 61661008, and Grant 11562004, in part by the Guangxi Natural Science Foundation under Grant 2017GXNSFAA198180 and Grant 2016GXNSFCA380017, in part by the Overseas 100 Talents Program of Guangxi Higher Education, in part by the 2018 Guangxi One Thousand Young and Middle-Aged College and University Backbone Teachers Cultivation Program, and in part by the Doctoral Research Foundation of Guangxi Normal University under Grant 2016BQ005.

ABSTRACT In this paper, a novel image watermarking method is proposed which is based on discrete wave transformation (DWT), Hessenberg decomposition (HD), and singular value decomposition (SVD). First, in the embedding process, the host image is decomposed into a number of sub-bands through multi-level DWT, and the resulting coefficients of which are then used as the input for HD. The watermark is operated on the SVD at the same time. The watermark is finally embedded into the host image by the scaling factor. Fruit fly optimization algorithm, one of the natural-inspired optimization algorithms is devoted to find the scaling factor through the proposed objective evaluation function. The proposed method is compared to other research works under various spoof attacks, such as the filter, noise, JPEG compression, JPEG2000 compression, and sharpening attacks. The experimental results show that the proposed image watermarking method has a good trade-off between robustness and invisibility even for the watermarks with multiple sizes.

INDEX TERMS Image watermarking, discrete wave transformation, singular value decomposition, Hessenberg decomposition, fruit fly optimization algorithm.

I. INTRODUCTION

The explosive growth of internet usage makes information dissemination become increasingly easier than ever, leading to serious copyright infringement problems, such as unauthorized copying [1], distribution [2], [3] and modification of digitized works [4], [5]. In order to improve the effective utilization of the network information, the copyright protection is becoming particularly important [1]. As one of the widely used protection techniques, watermarking method has been applied in many fields of multimedia copyright protection [1]–[5]. Watermarking is a common information embedding technique to protect the image, video and audio information. It integrates the key information into the modalities by invisibly modifying the data. Therefore, invisibility and robustness are two major metrics for evaluating the effectiveness of the watermarking techniques [1]. Based on

these two metrics, watermarking techniques can be broadly classified into three groups, i.e. the robust, fragile and semi-fragile watermarking [1]. The robust watermarking is crucial for the image data protection because it does not significantly reduce the visual quality of the watermarked image, and can withstand various attacks [2]. It is therefore widely used for copyright protection and ownership verification. Fragile watermarking is only used to ensure the completeness of the image rather than to verify actual ownership [2]. Even though it can detect any unauthorized modification or any modifications of the watermarked images, it also destroy the completeness of the watermark if any change happens. Semi-fragile watermarking combines the advantages of fragile watermarking and robust watermarking, with the aim to detect unauthorized manipulations while keeping the robustness against authorized manipulations [2].

As for the robust watermarking method, the watermark information is often directly embedded in the spatial domain, i.e. the watermark data is embedded into the host image by

The associate editor coordinating the review of this manuscript and approving it for publication was Huaqing Li.

modifying the pixels spatially [2]. This operation is easy to implement but it is not robust enough against the geometric and image processing attacks [2]. In the meantime, the embedding process can also be completed in the transformed domains, e.g. the discrete cosine transform (DCT) [6]–[11], discrete Fourier transform (DFT) [12]–[14], discrete wave transformation (DWT) [15]–[17], and singular value decomposition (SVD) [10], [11], [18]–[21]. To ensure the robustness of the embedding algorithms, frequency domain analysis is utilized to find out the possible locations of the embedding watermark coefficients [16], [22]. Research shows that the human vision is more sensitive to low and middle frequency coefficients [1]. Therefore, a good performance of the operation methods in the transformed domain can be achieved, especially when the watermarks are embedded within the low frequency ranges [1]. Moreover, it is reported that the DWT-based watermarking methods have the advantages of multi-resolution, good energy compression, and an imperceptible visual quality [15]–[17], thus it can be used for image watermarking. However, the DWT-based watermarking is difficult to resist geometric attacks [23]. This drawback can be addressed by extracting the geometric features of the image by using the matrix decomposition. Therefore, the method based on the DWT and matrix decomposition is widely used in the image watermarking to resist image processing and geometric attacks [23]–[25]. The most common matrix decompositions used in the watermarking include SVD and Hessenberg decomposition (HD). The SVD provides a general and quantitative view on the image changes, and its structural information is crucial in predicting the image quality. Note that the singular vectors can represent structural information. Modifications in singular vectors are linked to the singular values which primarily represent the image luminance. Based on this, some robust watermarking methods are introduced in [26]–[30], which are based on DWT and SVD. The major concern of the SVD-based watermarking methods is the false positive problem, which can be solved using the encryption operation. Specifically, the components of SVD are encrypted by the chaotic systems, which can guarantee the watermarking method having a strong security performance, i.e. the false positive problem is solved. The matrix decomposition of HD has also been widely used for watermarking [31], [32]. It provides a method to embed the watermarks. However, the aforementioned watermarking methods require that the size of watermark is fixed. The watermarking methods under various sizes of watermarks are still required to be investigated [33].

In addition, the performances of invisibility and robustness are two vital metrics for the image watermarking, and the trade-off between them is always a challenging. Recently, several bio-inspired algorithms are used to address this problem, such as differential evolution [34], artificial bee colony (ABC) [35], [36], firefly algorithm [37], [38], particle swarm optimization (PSO) [39], and fruit fly optimization algorithm (FOA) [40], [41]. In the approaches of [40]–[45], the FOA is used to solve the trade-off problem, and the performances

are improved. In this paper, FOA is employed to optimize the parameters of the proposed algorithm and a trade-off between the invisibility and robustness is achieved. Based on these discussions, a novel image watermarking algorithm which combines DWT, HD and SVD is proposed in this paper. The performance test shows that this method has good invisibility and robustness, and does not have the constraint of fixed sizes of watermarks. Specifically, this work exploits an objective evaluation function (OEF) and FOA to find an adaptive and optimal scaling factor to achieve a trade-off between invisibility and robustness. The main contributions of this work include: (1) The proposed watermarking method satisfies the multiple sizes of watermarks, and the trade-off between invisibility and robustness is achieved with a good performance; (2) OEF is proposed to assist in finding the optimal scaling factor to solve the contradiction between the invisibility and robustness, and FOA is employed to find the optimal factor; (3) HD is used to change the coefficients before SVD operation which can enhance the robustness of the watermarking; (4) Results show that the proposed watermarking method is robust under the attacks of filter, noise, JPEG compression, JPEG2000 compression and sharpening.

The remaining parts of this work are organized as follows. In Section II, the concepts about DWT, HD, SVD and FOA are provided. In Section III, the proposed watermarking method based on DWT-HD-SVD and FOA is detailed. Experimental results and performance analysis are given in Section IV. Section V gives the conclusion.

II. PRELIMINARIES

In this section, four techniques of DWT, HD, SVD and FOA are introduced which will be used in the proposed watermarking method. The time-scale signal multi-resolution of DWT can improve the watermarking performance under robustness attacks. In the meantime, when HD performs as the matrix transform, the robustness has a further improvement. In addition, the SVD-based watermarking method has a performance improvement when defending the geometric attacks (e.g. rescaling attack). However, the SVD-based watermarking has a major concern of false positive problem, which is solved by encrypting the SVD components in this work. Finally, during the development of the watermarking methods, the optimization should be performed, i.e. the trade-off between invisibility and robustness needs to be balanced. In this work, FOA will be used to address this optimization problem.

A. DISCRETE WAVE TRANSFORMATION

DWT is one of the popular mathematical transforms that has numerous applications in science and engineering [35]. It provides an energy compact representation of the image and has a good effect on the resistance of image processing attacks in the watermarking [17]. The host image is transformed into four sub-bands by DWT which include low-high (LH), high-low (HL), high-high (HH) and low-low (LL). Most of the

information contained in the host image is concentrated into the LL sub-band after one level of DWT. The wavelet theory makes it possible to operate further decomposition until the size of sub bands satisfies the requirement of watermark. Compared with other sub-bands, LL has a better performance on the attacks, e.g. filter, compression attacks [28], [30]. This characteristic makes the LL sub-band an excellent candidate for the robust watermarking [37].

B. HESSENBERG DECOMPOSITION

HD is a kind of matrix decompositions which can be used for square matrix decomposition [32]. A $n \times n$ square matrix X can be decomposed by using HD as shown by

$$PHP^T = \text{HD}(X), \quad (1)$$

where P is an orthogonal matrix and H is an upper Hessenberg matrix, and $h_{i,j} = 0$ when $i > j + 1$. HD is typically computed by the Householder matrices. Householder matrix Q is an orthogonal matrix and it is expressed as

$$Q = (I_n - 2\mu\mu^T)/\mu^T\mu, \quad (2)$$

where μ is a non-zero vector in R^n , and I^n is a $n \times n$ identity matrix. There are $n - 2$ steps in the overall procedure. Therefore, HD is computed as

$$P = (Q_1 Q_2 \dots Q_{n-2})^T X (Q_1 Q_2 \dots Q_{n-2}) \quad (3)$$

$$\Rightarrow H = P^T X P, \quad (4)$$

$$\Rightarrow X = PHP^T. \quad (5)$$

The robustness is improved because a more precise component of the host image can be found by HD [31], [32].

C. SINGULAR VALUE DECOMPOSITION

SVD decomposes a symmetric matrix into three sub-matrices in such a way that singular values get separated in the form of diagonal matrix [46]. The three decomposed matrices are left singular matrix U , singular matrix S and right singular matrix V under the matrix diagonalization. Suppose Y is a symmetric matrix then SVD can be computed by

$$USV^T = \text{SVD}(Y) \quad (6)$$

where $UU^T = I_n$ and $VV^T = I_n$. The columns of U are orthonormal eigenvectors of YY^T , the columns of V are orthonormal eigenvectors of $Y^T Y$ and S is a diagonal matrix that contains the square roots of the eigenvalues from U or V in descending order. If $r(r \leq n)$ is the rank of the matrix Y then the elements of the diagonal matrix S can satisfy relation in Eq. 7, and the matrix Y can be written as Eq. 8.

$$\begin{aligned} \sigma_1 &\geq \sigma_2 \geq \dots \geq \sigma_r \geq \sigma_{r+1} \\ &= \sigma_{r+2} = \dots = \sigma_n = 0, \end{aligned} \quad (7)$$

$$Y = \sum_{i=1}^r \sigma_i \mu_i \nu_i^T, \quad (8)$$

where μ_i, ν_i are the i_{th} eigenvector of U and V , σ_i is the i_{th} singular value. The singular value S of SVD is used in this work, the singular value of the watermark is embedded into the host image by a suitable scaling factor. After this operation, the invisibility and the robustness of the watermarking algorithm is roughly complete, as the scaling factor is not suitable, the precise performance of the proposed algorithm is needed to be improved. Therefore, the trade-off of the invisibility and robustness is needed further to be optimized by the proposed evaluation function. As the other components of SVD, U and V^T , would provide the geometric information in the extraction process, when they are not be protected which could cause the major concern in the SVD-based watermarking, and this concern is solved by encrypting U and V^T .

D. FRUIT FLY OPTIMISATION ALGORITHM

FOA is a biomimetic optimization algorithm. It is proposed in the approach of [40] which is inspired by the flashing behavior of fruit fly, and it works like a signal system which aims to attract other fruit flies. The optimization problem can be solved by the biomimetic algorithms, i.e. genetic algorithm, ABC, differential evaluation, ant colony optimization algorithm and PSO. However, the common disadvantages of these algorithms are complicated computational processes, and very many parameters in these methods [40]. The characteristics of FOA are the simple implementation and better global optimization ability. The algorithm of FOA can be summarized as follows.

- *Step 1.* Initialize the position of the fruit fly swarm locations randomly, and it is denoted as X_a, Y_a .
- *Step 2.* Compute the random direction and distance of an individual fruit fly based on its behavior of searching food using smell. It is denoted as $X_i = X_b + x_r$, $Y_i = Y_b + y_r$, where x_r and y_r are the random values, X_b and Y_b are the location coordinates, whose initial values are X_a, Y_a .
- *Step 3.* Because the food location is not known, the distance D_i to the origin is firstly estimated, which is denoted as $D_i = \sqrt{X_i^2 + Y_i^2}$, then the value of smell concentration S_i is calculated. The value is the reciprocal of distance, which is denoted as $S_i = 1/D_i$.
- *Step 4.* Find the smell concentration $Smell_i$ of the individual location of the fruit fly, S_i is substituted by the smell concentration judgment function, and it is denoted as $Smell_i = \text{Function}(S_i)$.
- *Step 5.* Find out the maximal smell concentration in the fruit fly swarm, and it is denoted as $[bestSmell, bestIndex] = \max(Smell_i)$.
- *Step 6.* Record the best smell concentration value and the coordinate, then the fruit fly swarm will fly towards the final location using vision $Smell_{best} = bestSmell$, $X_b = X(bestIndex)$, $Y_b = Y(bestIndex)$.

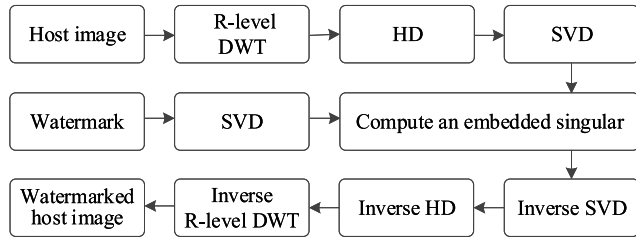


FIGURE 1. Procedure of the watermarking embedding.

- Step 7. Enter iterative optimization to repeat Steps 2-5 when the iterative smell concentration is superior to the previous. Otherwise, return to Step 6.

III. PROPOSED WATERMARKING SCHEME

In this section, the watermarking embedding algorithm is introduced in Section III-A and the watermarking extraction algorithm is introduced in Section III-B. In addition, Section III-C presents how to achieve a trade-off between the invisibility and robustness using FOA, i.e. using FOA to find the optimal scaling factor in the proposed watermarking method.

A. WATERMARKING EMBEDDING ALGORITHM

The host image C and the watermark W are the input in the watermarking embedding algorithm, and the output is watermarked host image C^* . The sizes of C , W , C^* are $M \times M$, $N \times N$ and $M \times M$, respectively. In addition, this watermarking method can accommodate watermarks with multiple sizes, and the host image is decomposed by R-level DWT. The procedure of the watermarking embedding is shown in Fig. 1 and the detailed embedding steps are specified in the following steps.

- Step 1. Based on R-level DWT, C is decomposed into the components of LL , LH , HL , HH , where $R = \log_2 \frac{M}{N}$.
- Step 2. HD is performed on LL , and it is shown as

$$PHP^T = HD(LL). \quad (9)$$

- Step 3. Apply SVD to H

$$HU_w HS_w HV_w^T = SVD(H). \quad (10)$$

- Step 4. W is applied with SVD, i.e.

$$U_w S_w V_w^T = SVD(W). \quad (11)$$

Then the operation of U_w , V_w^T is encrypted by the chaotic system which is generated by the Logistic map. This specified encryption is detailed in the experimental analysis of false positive problem. The encrypted two components are marked as U_{w1} and V_{w1}^T .

- Step 5. Compute an embedded singular value HS_w^* by adding HS_w and S_w with a scaling factor α by

$$HS_w^* = HS_w + \alpha S_w. \quad (12)$$

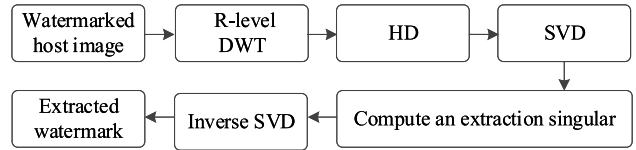


FIGURE 2. Procedure of the watermarking extraction.

- Step 6. The watermarked sub-band H^* is generated by using the inverse SVD, i.e.

$$H^* = HU_w HS_w^* HV_w^T. \quad (13)$$

- Step 7. A new low-frequency approximate sub-band LL^* is reconstructed based on the inverse HD which is given by

$$LL^* = PH^* P^T. \quad (14)$$

- Step 8. The watermarked image C^* is obtained by performing the inverse R-level DWT.

B. WATERMARKING EXTRACTION ALGORITHM

In the watermarking extraction algorithm, the input is the watermarked host image C^* , and the output is extracted watermark W^* . The size of W^* is $N \times N$. The procedure of the watermarking extraction is shown in Fig. 2 and the detailed extracting steps are shown as follows.

- Step 1. The watermarked host image C^* is decomposed into four sub-bands by R-level DWT, which include LL_w , LH_w , HL_w , HH_w .
- Step 2. HD is performed on LL_w by

$$P_w H_w P_w^T = HD(LL_w). \quad (15)$$

- Step 3. Apply SVD to H_w , i.e.

$$HU_w^* HS_w^* HV_w^{*T} = SVD(H_w). \quad (16)$$

- Step 4. The extracted singular value S_w^* is gained by

$$S_w^* = (HS_b^* - HS_w^*)/\alpha. \quad (17)$$

- Step 5. The components U_{w1} and V_{w1}^T are decrypted by the chaotic system. Then the decrypted two components are marked as U_{w2} and V_{w2}^T . The extracted watermark W^* is reconstructed by inverse SVD, which is described by

$$W^* = U_{w2} S_w^* V_{w2}^T. \quad (18)$$

C. ALGORITHM OPTIMIZATION USING FOA

As one of the swarm intelligence optimization algorithms, FOA is used to solve the trade-off problem between the invisibility and robustness in this work. Invisibility is generally measured by the performance metrics such as peak signal to

noise ratio (PSNR) and structural similarity index measure (SSIM). PSNR is defined by

$$\text{PSNR}(C, C^*) = 10 \lg \frac{C_{\max}^2}{\text{MSE}}, \quad (19)$$

$$\text{MSE} = \frac{1}{M^2} \sum_{i=1}^M \sum_{j=1}^M (C_{i,j} - C_{i,j}^*)^2, \quad (20)$$

where MSE is the mean square error between host image and watermarked host image and C_{\max} is the maximum pixel value in the host image. SSIM is defined by

$$\text{SSIM}(C, C^*) = \frac{\mu_C \mu_{C^*} + d_1}{\mu_C^2 + \mu_{C^*}^2 + d_1} \cdot \frac{\sigma_{CC^*} + d_2}{\sigma_C^2 + \sigma_{C^*}^2 + d_2}, \quad (21)$$

where μ_C and μ_{C^*} are the average of C and C^* , σ_C^2 and $\sigma_{C^*}^2$ are the variance of C and C^* , σ_{CC^*} is the covariance of C and C^* , d_1 and d_2 are two variables which are used to stabilize the division with a weak denominator.

Normalized correlation (NC) is often used to evaluate the robustness of the original and extracted watermarks, which is defined by

$$\text{NC} = \frac{\sum_{i=1}^N \sum_{j=1}^N W_{i,j} W_{i,j}^*}{\sqrt{\sum_{i=1}^N \sum_{j=1}^N W_{i,j}^2} \sqrt{\sum_{i=1}^N \sum_{j=1}^N W_{i,j}^{*2}}}, \quad (22)$$

With an assumption that K types of attacks are applied in the watermarked host image, OEF is defined to optimize the scaling factor, which is given by

$$\begin{aligned} \text{OEF}(\alpha_i, \lambda, \omega_i) \\ = \omega_1 \frac{1}{\lambda} \text{PSNR}(C, C^*) \\ + \omega_2 \text{SSIM}(C, C^*) + \omega_3 \frac{\sum_{i=1}^K \text{NC}(W, W_i^*)}{K}, \end{aligned} \quad (23)$$

where W_i^* is the extracted watermark under i_{th} attack, $\alpha_i (i = 1, 2, \dots, t)$ is the scaling factor array and t is the maximum number index in the scaling factor array, λ is the weight factor, $\omega_1, \omega_2, \omega_3$ are the proportion coefficients which directly reflect the proportion of invisibility or robustness, K represents the amount of attacks.

The details of the proposed OEF are described as follows. (a). ω_1, ω_2 and ω_3 denote the quantization coefficients of invisibility or robustness, and they are adjustable. (b). Normalization of PSNR (PSNR/λ): when $\text{PSNR} > 37\text{dB}$, the image quality is acceptable [38]. When the weight factor λ is 37, PSNR/λ is normalized to $[0, 1)$ and $[1, \text{PSNR}(C, C^*)/37]$, where $[0, 1)$ means that the invisibility of the watermarking is not acceptable, and $[1, \text{PSNR}(C, C^*)/37]$ means that the invisibility of the watermarking is acceptable. (c). Using PSNR and SSIM as the evaluation of invisibility: PSNR and SSIM can evaluate the image quality from two aspects. The two proportion coefficients ω_1, ω_2 are used to reconcile them. The detailed steps to find the optimal scaling factor in the proposed watermarking method are introduced below, where the corresponding flow chart is shown by Fig. 3 and the pseudo-code is shown in Algorithm 1.

- *Step 1.* Initialize parameters in OEF and FOA. The parameters of OEF include the scaling factor array $\alpha_i (i = 1, 2, \dots, t)$, the weight factor λ and the proportion coefficients $\omega_i (i = 1, 2, 3)$. X_a and Y_a are the initialization of FOA and they denote the fruit fly population location. MG denotes the maximum number of iterations, and SP denotes the size of fruit fly population.
- *Step 2.* The values of OEF are calculated as following steps. (a). According to the procedure of watermarking embedding shown in Fig. 1, the watermarked host image C^* can be obtained by using the host image C and watermark W with α_i . (b). Apply K different types of attacks on the watermarked host images. Based on the watermarked images, the extracted watermark W_i^* can be obtained by using the procedure of watermarking extraction in Fig. 2. (c). Compute $\text{PSNR}(C, C^*)$, $\text{SSIM}(C, C^*)$ and $\text{NC}(W, W_i^*)$ based on the results of previous step of (a) and (b). (d). Calculate OEF values of each location based on Eq. 23, and the calculated values are prepared for the smell concentration judgment function in Step 3. (c)
- *Step 3.* Use FOA to get the optimal scaling factor. (a). The distance for searching food based on an individual fruit fly is denoted as $X_i = X_b + x_r, Y_i = Y_b + y_r$. (b). Estimate distance and smell concentration judgment value, which are denoted by $D_i = \sqrt{X_i^2 + Y_i^2}$ and $S_i = 1/D_i$. (c). Smell concentration judgment function among fruit fly swarm is $\text{Smell}_i = \text{Function}(S_i)$, where $\text{Function}(S_i)$ is based on OEF. (d). Find out the fruit fly with maximal smell concentration among fruit fly swarm, and it is denoted as $[\text{bestSmell}, \text{bestIndex}] = \max(\text{Smell}_i)$. (e). Record the best smell concentration value and coordinate using $\text{Smellbest} = \text{bestSmell}$, $X_b = X(\text{bestIndex})$, and $Y_b = Y(\text{bestIndex})$. (f). Repeat previous steps between (a) and (e) until the maximum iteration (denoted by MG) is reached then the optimal scaling factor is marked as the result. Otherwise, update the fruit fly population location when the iterative smell concentration is superior to the previous smell concentration.

IV. EXPERIMENTAL RESULTS AND ANALYSIS

In this section, the invisibility and robustness of the proposed method are analyzed. Firstly, the optimal adaptive scaling factor of watermarks with multiple sizes is found through the analysis of scaling factor over NC, PSNR and SSIM. Then the adaptive optimal scaling factors of watermarks with multiple sizes are used in the experiments. The invisibility and robustness of the proposed method are detected by subjective visual observation and objective quantitative analysis. Moreover, various attacks with different parameters are used to further evaluate the robustness. Finally, the invisibility and robustness of the proposed method are compared with the related works.

All the experiments are conducted on a computer with an Intel dual core 3.7 GHz CPU with 8.0 GB RAM, where the

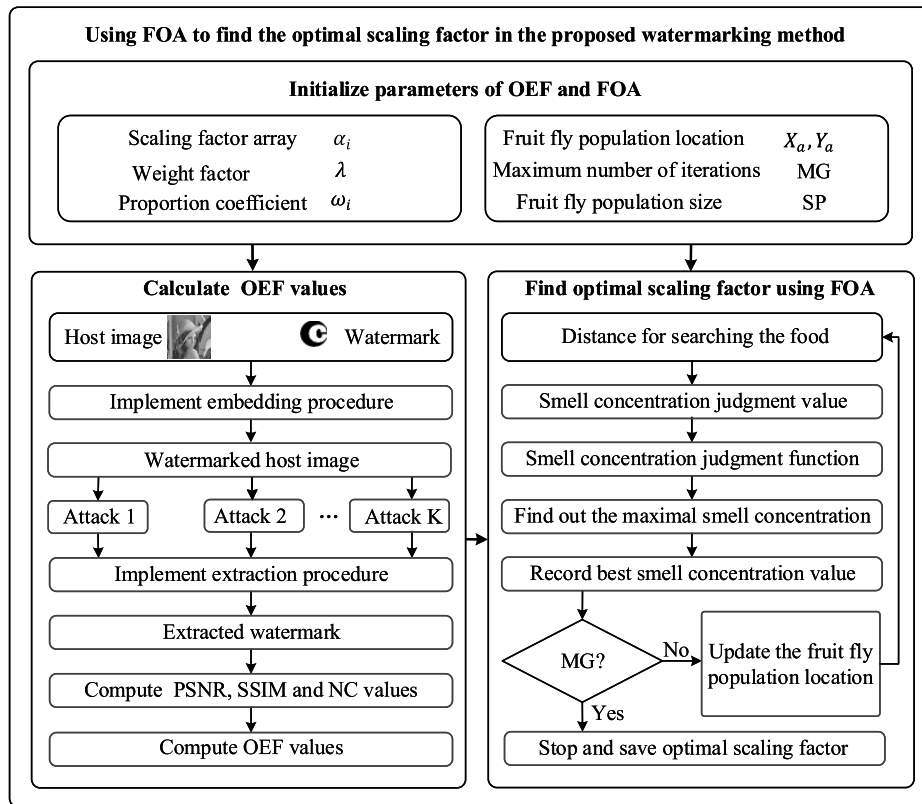


FIGURE 3. Scaling factor optimization using FOA.

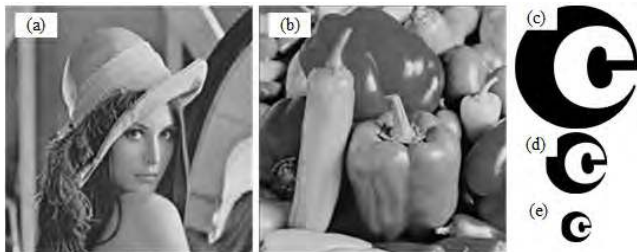


FIGURE 4. Host images: (a) Lena, (b) Pepper. Watermark images: (c-e) 256×256 , 128×128 , 64×64 sizes of “copyright”.

MATLAB version R2017a is used. The host images with 512×512 size in the experiments are shown in Fig. 4(a-b). These two host images (Lena and Pepper) are the most popular test images, and other images are also tested in this work which have similar results. In order to have a fair performance comparison, the results of using Lena and Pepper as the host images are provided in this section. Grayscale images “copyright” with sizes of 256×256 , 128×128 , and 64×64 are used as the watermark images, and they are shown in Fig. 4 (c-e). All experiments are carried out under the conditions where the initial population size of the fruit fly is 20 and the maximum iteration is 100. These parameters are empirically selected in this work, and they can be further optimized using Minitab or other similar methods.

The performance of the proposed method is evaluated by different experiments. Various attacks shown in Table 1

are used to test the robustness. Watermarked images suffers the attacks. The attacks include the filter, noise, cropping, compression, rescaling, histogram equalization (HE), motion blur, sharpening and rotation attacks. Specifically, the filter attacks use the wiener, median, Gaussian low-pass and average filters. The noise attacks are based on Gaussian, salt & peppers and speckle noises. The compression attacks include JPEG and JPEG2000 attacks. Rescaling attack includes rescaling (shrink) and rescaling (enlarge). The parameters in these attacks are set by: filter with 3×3 window size, noise addition with 0.001 density or variance, cropping with 2% cropping percentage, JPEG compression with quality factor (QF) 50, JPEG2000 compression with compression ratio (CR) 12, rescaling with rescaling coefficients 0.25 and 4, motion blur with Theta=4, Len=7, sharpening with threshold 0.8 and rotation with angle 2 degree.

A. FINDING THE OPTIMAL SCALING FACTOR

In the proposed watermarking algorithm, the performance can achieve an optimal state if the optimal factor is found. According to Section III-C, an optimal t for the watermarks with multiple sizes needs to be decided and taken back to OEF, then the optimal scaling factor is calculated. As an example, the 64×64 watermark and 512×512 Lena are selected to find the optimal t by investigating the relationship between the scaling factor and the evaluation parameters. The curve of $NC(W, W^*)$ values with the scaling factor under

Algorithm 1 Using FOA to Find the Optimal Scaling Factor

Input: Scaling factor array, $\alpha_i (i = 1, 2, \dots, t)$; Weight factor, λ ; Proportion coefficient, $\omega_i (i = 1, 2, 3)$; Fruit fly population location, X_a, Y_a ; Maximum number of iterations, MG; Fruit fly population size, SP; Host image, C ; Watermark, W ;

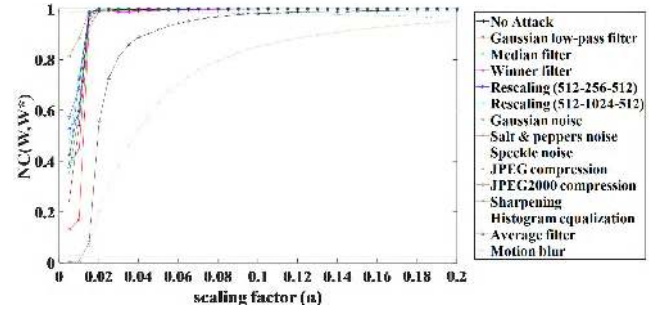
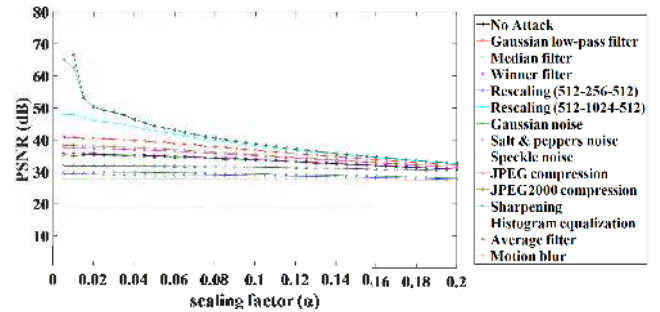
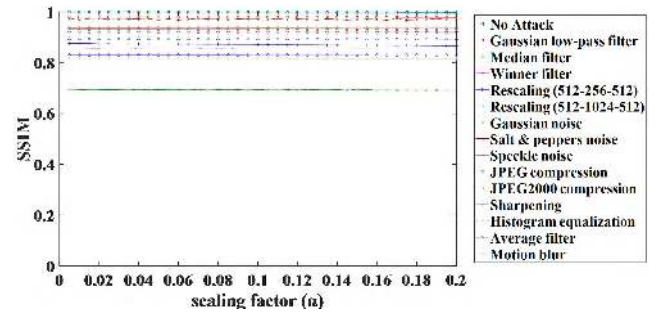
Output: Optimal scaling factor, α ;

- 1: Implement embedding procedure;
- 2: Gain watermarked host image C^* ;
- 3: Perform K robustness attacks;
- 4: Implement extraction procedure;
- 5: Gain the extracted watermarks W_i^* ;
- 6: Compute PSNR, SSIM and NC values;
- 7: Compute OEF values;
- 8: Compute the distance for searching the food;
- 9: Compute the smell concentration judgment value;
- 10: Gain the smell judgment function based on OEF;
- 11: Find the maximal smell concentration;
- 12: Record the best smell concentration;
- 13: Determine if MG is reached. If yes, then stop and save the optimal scaling; otherwise update the fruit fly population location;
- 14: **return** α ;

TABLE 1. Different attacks used in the experiments.

Attack	Specification
Filter attack	Wiener filter (3×3)
	Median filter (3×3)
	Gaussian low-pass filter (3×3)
	Average filter (3×3)
Noise attack	Gaussian noise ($V=0.001$)
	Salt & peppers noise (0.001)
	Speckle noise (0.001)
Cropping attack	Cropping percentage (2%)
Compression attack	JPEG compression (QF=50)
	JPEG2000 compression (CR=12)
Rescaling attack	Rescaling (0.25)
	Rescaling (4)
HE attack	HE
Motion blur attack	Motion blur (Theta=4, Len=7)
Sharpening attack	Sharpening (0.8)
Rotation attack	Angle (2 degree)

various attacks is given in Fig. 5. NC values vary in the range of $[0.005, 0.2]$, and get stabilized in the range of $[0.015, 0.2]$, but the convergence rates of average filter and motion blur are slower than others. This is specifically true for all attacks except HE. For HE, NC values decrease in the range of $[0.005, 0.2]$. Therefore, it is good to set the start value of t for NC by $t_1 = 0.015$. The curves of $PSNR(C, C^*)$ and $SSIM(C, C^*)$ with scaling factor are shown in Fig. 6 and Fig. 7, respectively. PSNRs with α are negative correlations with the range of $[0.005, 0.2]$. SSIMs are almost constant with the range of $[0.005, 0.2]$. Therefore, for $PSNR(C, C^*)$ and $SSIM(C, C^*)$, the start values of t are set as $t_2 = [0, 0.02]$ and $t_3 = [0, 0.2]$.

**FIGURE 5.** NCs under different scaling factors.**FIGURE 6.** PSNRs under different scaling factors.**FIGURE 7.** SSIMs under different scaling factors.

Therefore, t is calculated by $t = (t_{max} - t_s)/p$, where $t_{max} = 0.2$, $t_s = t_1 \cap t_2 \cap t_3$, p is the minimum interval. Then it is taken back to OEF, and the optimal scaling factor can be obtained. Similarly, the adaptive scaling factors for the other sizes of watermarks can be found.

B. INVISIBILITY AND ROBUSTNESS ANALYSIS

The watermarked host image should be invisible to humans to ensure the safety of information, hence the watermark invisibility is an important metric to measure the performance. The baseline must be established while the watermarked images do not suffer attacks. Fig. 8 shows the watermarked host images which suffered no attack and the corresponding extracted watermarks with watermark sizes of 256×256 , 128×128 , 64×64 . The PSNRs, SSIMs and the NCs are listed in Fig. 8. Generally, if $PSNR > 37\text{dB}$, the watermarked image is acceptable and thus the watermark is invisible to human visual system. Moreover, when $SSIM > 0.93$, the watermarked image has a small difference with the host image [38].

Watermark size	256 × 256		128 × 128		64 × 64	
Host image	Lena	Peppers	Lena	Peppers	Lena	Peppers
Watermarked host image						
PSNR (dB)	38.1621	38.1295	38.1625	38.1539	38.2477	38.2178
SSIM	0.9992	0.9989	0.9992	0.9990	0.9991	0.9989
Extracted watermark						
NC	1.0000	1.0000	1.0000	1.0000	1.0000	1.0000

FIGURE 8. Invisibility performance: Watermarked images and corresponding extracted watermarks with various sizes and their corresponding PSNRs, SSIMs and NCs.

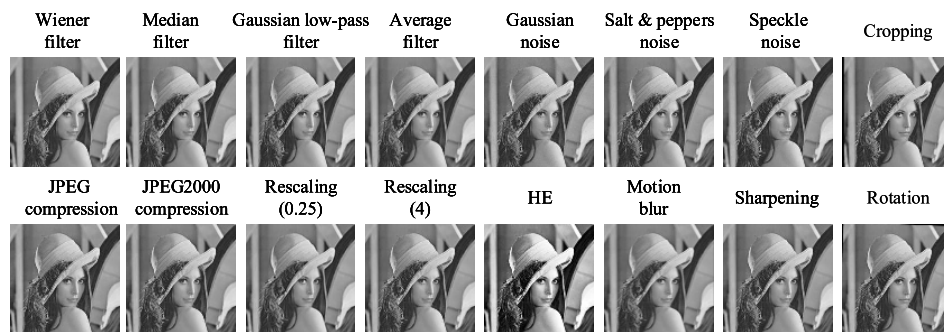


FIGURE 9. Attacked watermarked Lena with 64 × 64 watermark.

According to Fig. 8, the invisibility performance of the proposed method is that all PSNRs and SSIMs are greater than 38dB and 0.9989, respectively. NCs of the extracted watermarks are all 1.0000 when the watermarked host images do not suffer attack. It shows that the watermarking method has good invisibility. Hence the proposed method meets the requirements of watermarking invisibility in both the subjective and objective analysis.

The robustness needs to be further evaluated when the invisibility is acceptable. Robustness indicates the ability of a system to resist any change without adapting its initial stable configuration. In image watermarking method, robustness is the ability to extract watermarks from the watermarked host images under various attacks. Therefore, it is important to verify the robustness for an image watermarking method. In order to evaluate the robustness of the proposed method, the quality of the extracted watermarks is verified when the watermarked images suffer various attacks. Besides, the objective evaluation of the extracted watermarks is also tested. Specifically, several cases are that the watermarked images are suffered the attacks with 64 × 64 watermark which are shown in Fig. 9. By using the extraction algorithm, the extracted watermarks are obtained. The same execution is done for the 256 × 256 and 128 × 128 watermarks. The extracted watermarks and corresponding values for the

watermarks with three cases are listed in Fig. 10. As shown in Fig. 10, it can be seen that not only the visual quality of the extracted watermarks is acceptable, but also NCs are relatively high in this work. Specifically, NCs of all attacks except for HE become larger as the size of watermark is smaller, i.e. from 256 × 256, 128 × 128 to 64 × 64. Besides, NCs of the attacks except for motion blur are larger than 0.9 for three watermarks. In addition, almost the extracted watermarks of these attacks are visually clear, and even though the extracted watermarks of the motion blur are slightly blurred, the main information of the watermarks is still identifiable. For the three sizes of watermark, i.e. 256 × 256, 128 × 128, 64 × 64, when defend the four filter attacks, the NCs are 0.92, 0.95, 0.99, respectively. For the three noise attacks, the NCs are all 0.99. For the two compression attacks, the NCs are all 0.99. For the rescaling attacks, the NCs are 0.96, 0.97, 0.99. For HE, the NCs are all 0.99. For the motion blur, the NCs are 0.83, 0.85, 0.91. For the sharpening attack, the NCs are all 1. Besides, the watermarks with three sizes, i.e. 256 × 256, 128 × 128, 64 × 64 are chosen to test to defend the cropping attack, and the test results show that NCs are all larger than 0.97. The NC values of the rotation attack are all larger than 0.93. Therefore, it illustrates that the proposed watermarking method has high robustness to defend filter, noise, compression, and sharpening attack.














































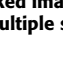
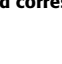
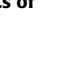
Attacks	256×256	128×128	64×64
Wiener filter	 0.9682	 0.9880	 0.9979
Median filter	 0.9685	 0.9905	 0.9993
Gaussian low-pass filter	 0.9749	 0.9973	 0.9992
Average filter	 0.9294	 0.9539	 0.9911
Gaussian noise	 0.9864	 0.9987	 0.9997
Salt & peppers noise	 0.9985	 0.9996	 0.9997
Speckle noise	 0.9981	 0.9998	 0.9998
Cropping	 0.9823	 0.9785	 0.9760
JPEG compression	 0.9998	 0.9999	 0.9997
JPEG2000 compression	 0.9997	 0.9999	 0.9998
Rescaling (0.25)	 0.9269	 0.9745	 0.9995
Rescaling (4)	 0.9999	 1.0000	 1.0000
HE	 0.9924	 0.9911	 0.9878
Motion blur	 0.8322	 0.8569	 0.9147
Sharpening	 1.0000	 1.0000	 1.0000
Rotation	 0.9496	 0.9422	 0.9306

FIGURE 10. Robustness performance: Extracted watermarks from the attacked watermarked images Lena and corresponding NCs of watermarks with multiple sizes.

The parameters in the above test attacks are static, and in order to further reflect the robustness of the proposed method, the case of dynamic parameters should be considered as well. The experiments with dynamic parameters are executed and tested, and the corresponding results in Fig. 11. In Fig. 11(a), the robustness is tested under JPEG compression with different QFs which are varied from 90 to 10 with a step of -10 , in which QF indicates the compression strength. The smaller the QF, the more the image is compressed. In the case of the watermarks with three sizes, NCs slowly decrease. Even when the QF reaches at 10, the NCs are all larger than 0.9965. Fig. 11(b) displays the experiments under

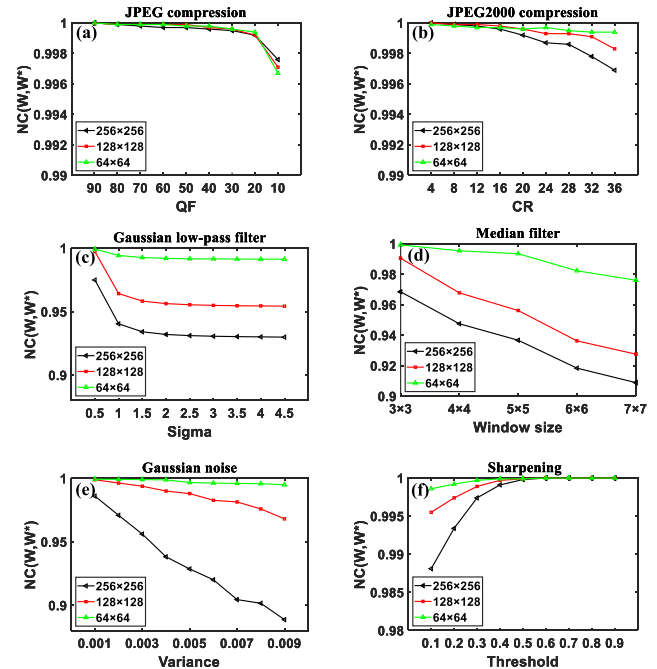


FIGURE 11. NC values under different parameters suffering various attacks. (a) JPEG compression, (b) JPEG2000 compression, (c) Gaussian low-pass filter, (d) median filter, (e) Gaussian noise, and (f) sharpening.

JPEG2000 compression attack with CRs selected from 4 to 36 with a step of 4. The larger the CR, the more image is compressed. For the three watermarks, even when the CR value is 36, the worst NCs of the three watermarks are larger than 0.9995, 0.9980, and 0.9970, respectively. In Fig. 11(c) and (d), the robustness is tested under Gaussian low-pass filter and median filter, and the parameters are positive standard deviation sigma set from 0.5 to 4.5 with a step of 0.5 and window size set from 3×3 to 7×7 with a step of 1×1 . The test results show that NCs of Gaussian low-pass filter are all larger than 0.93 for the three watermarks. Especially for 64×64 watermark, the NCs are larger than 0.99. With the increasing of the window size, NCs of the median filter are all larger than 0.91 for the three watermarks. NCs of the median attack attain 0.98 for 64×64 watermark as well. The cases of Gaussian noise and sharpening are tested with the varied variance and threshold, and the results are shown in Fig. 11 (e) and (f). Their setting ranges are $[0.001, 0.009]$ with a step of 0.001 and $[0.1, 0.9]$ with a step of 0.1, respectively. NCs of the Gaussian noise and sharpening are all larger than 0.8880 and 0.9880, respectively. Especially for 64×64 watermark, NCs for Gaussian noise and sharpening are all larger than 0.9900. Moreover, NCs of 64×64 watermark for the six attacks are all achieved to 0.98. As well known, the good NC value embodies high robustness to defend the six attacks even for the watermarks with different sizes, especially for JPEG compression, JPEG2000 compression and sharpening attack. Therefore, from the above analysis, it can be seen the proposed watermarking method has good invisibility and robustness.

C. FALSE POSITIVE PROBLEM (FPP) ANALYSIS

FPP is the major concern in the SVD-based watermarking, where a counterfeit watermark would be considered as the original watermark. Therefore, the components of the watermark image U and V^T of SVD are encrypted to solve this problem in this work, that is, an attacker with counterfeit U and V^T could only extract a random-like watermark. The specific encryption process of U and V^T includes the quantization mapping ($f : U_0 \leftarrow U, V_0^T \leftarrow V^T$) and the XOR operation with the Logistic map-based vectors. The definition of f is expressed by

$$f : \begin{cases} U_0(i, j) = R((U(i, j) - x_{\min}) \times \frac{y_{\max} - y_{\min}}{x_{\max} - x_{\min}}) \\ V_0^T(i, j) = R((V^T(i, j) - x_{\min}) \times \frac{y_{\max} - y_{\min}}{x_{\max} - x_{\min}}), \end{cases} \quad (24)$$

where R is the round operation, that is, the element is rounded to the nearest integer. $U(i, j)$ is the original value in vector U , $U_0(i, j)$ is the quantized value of U , $V^T(i, j)$ is the original value in vector V^T , $V_0^T(i, j)$ is the quantized value of V^T , x_{\max} , x_{\min} and y_{\max} , y_{\min} are the maximum and minimum values in vectors U and V^T , respectively. Besides, y_{\max} is set as 1000, and y_{\min} is set as 0. Hence, the ranges of U_0 and V_0^T are $[y_{\min}, y_{\max}]$. Then iterate the Logistic map to get two vectors x and y , and map them to range of $[y_{\min}, y_{\max}]$ by

$$\begin{cases} x(i+1) = ((\mu_1 x(i)(1 - x(i))) \times 10^{14} \bmod y_{\max} \\ y(i+1) = ((\mu_2 y(i)(1 - y(i))) \times 10^{14} \bmod y_{\max}, \end{cases} \quad (25)$$

where the initial parameters of $x(i)$, $y(i)$ are set as x_{01} , y_{01} , μ_1 , μ_2 . Then transform the one-dimensional vectors of x , y into two $N \times N$ form vectors U_{LM} and V_{LM} , and get the encrypted vectors U_1 and V_1^T by

$$\begin{cases} U_1 = \text{XOR}(U_0, U_{LM}) \\ V_1^T = \text{XOR}(V_0^T, V_{LM}), \end{cases} \quad (26)$$

The decryption process is the inverse process. In the experiment of FPP, a 64×64 watermark is selected shown in Fig. 12(a), and Fig. 12(b) is the extracted watermark with correct parameters $\mu_1, x_{01}, \mu_2, y_{01}$, and NC is 1.0000. Fig. 12(c) is the extracted watermark with correct parameters μ_1, x_{01} and wrong parameters μ_2, y_{01} , and NC is 0.5227. Fig. 12(d) is the extracted watermark with correct parameters μ_2, y_{01} and wrong parameters μ_1, x_{01} , and NC is 0.4794. Fig. 12(e) is the extracted watermark with wrong parameters $\mu_1, x_{01}, \mu_2, y_{01}$, and NC is 0.5025. From the Fig. 12 it can be seen, the extracted watermarks are like random-like watermarks with the wrong parameters. Moreover, when against the forged watermarks as well, the extracted watermarks also like the random-like watermarks. Therefore, FPP can be avoided in the proposed algorithm.

D. PERFORMANCE COMPARISON WITH RELATED WORKS

In this section, the proposed method is compared with the approaches using the bio-inspired algorithms including an ABC-based watermarking [35], the firefly

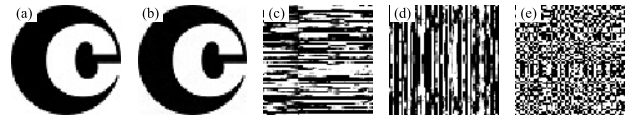


FIGURE 12. FPP result: (a) Original watermark. (b) Extracted watermark with correct parameters $\mu_1, x_{01}, \mu_2, y_{01}$, and NC = 1.0000. (c) Extracted watermark with correct parameters μ_1, x_{01} and wrong parameters μ_2, y_{01} , and NC = 0.5227. (d) Extracted watermark with correct parameters μ_2, y_{01} and wrong parameters μ_1, x_{01} , and NC = 0.4794. (e) Extracted watermark with wrong parameters $\mu_1, x_{01}, \mu_2, y_{01}$, and NC = 0.5025.

TABLE 2. NCs comparison with that in [35].

Attacks	[35]	In this work
Attack free	1.0000	1.0000
Median filtering (3×3)	0.9734	0.9685
Gaussian low-pass filter (3×3)	0.9784	0.9749
Gaussian noise ($M=0, V=0.005$)	0.8018	0.9286
Salt & peppers noise (0.001)	0.9783	0.9985
JPEG compression (QF=40)	0.9808	0.9998
JPEG compression (QF=50)	0.9852	0.9998
HE	0.9739	0.9924
Sharpening (0.8)	0.9239	1.0000

TABLE 3. NCs comparison with that in [37].

Attacks	[37]	In this work
Attack free	1	1
JPEG compression (QF=95)	1	1
3×3 Gaussian filter with deviation 0.5	0.9910	0.9992
Sharpening (0.2)	0.9957	0.9992
HE	0.9940	0.9878
Rescaling (4)	1	1

algorithm-based watermarking [37], [38], and a FOA-based watermarking [41]. Firstly, this work is compared with the method in which uses the swarm intelligence optimization algorithm ABC. The comparison of robustness is shown in Table 2 when the sizes of host image and the watermark are 512×512 and 256×256 . Table 2 shows that for the median/Gaussian filtering attacks, NCs of the proposed method are slightly lower than [35]. However, the NCs are better than [35] under other attacks (especially the noise, compression, HE and sharpening attacks), which indicates that the proposed method has a stronger overall robustness than [35].

Another comparison with [37], [38], [41] is carried out under the condition of 512×512 host image and 64×64 watermark, and the comparison results of NC are listed in Table 3, Table 4 and Table 5, respectively. According to the NCs in Table 3 and Table 4, the NCs of 3×3 Gaussian filter with a 0.5 standard deviation and sharpening (0.2) are better than those in [37], and the NCs of the Gaussian noise (0.002) and salt & peppers noise(0.001) are superior to those in [38]. Besides, for the attack free, JPEG (95), and rescaling (4), the NCs are the same as those in [37], and for the rescaling (0.25), JPEG compression (25), Gaussian low-pass filter (3), and 4×4 median filter, the NCs are slightly

TABLE 4. NCs comparison with that in [38].

Attacks	[38]	In this work
Rescaling(512 \rightarrow 256 \rightarrow 512)	1	0.9995
JPEG compression (QF=25)	1	0.9994
Gaussian noise with variance 0.002	0.9920	0.9992
Salt and peppers noise with density 0.001	0.9975	0.9997
3 \times 3 Gaussian filter with deviation 3	1	0.9915
4 \times 4 median filter	1	0.9954
HE	0.9910	0.9878

TABLE 5. NCs comparison with that in [41].

Attacks	[41]	In this work
JPEG compression (QF=70)	0.9993	0.9999
Gaussian noise with variance 0.001	0.9833	0.9997
3 \times 3 median filter	0.9933	0.9989

less than those in [38], but they are still in a similar level. According to the NCs in Table 5, the NCs of JPEG compression (QF=70), Gaussian noise(0.001) and 3 \times 3 median filter is better than that in [41]. Therefore, the overall performance of the proposed watermarking method is good, that is, almost better than those in [37], [38] and [41] in most situations, and it is especially robust to defend the JPEG compression attack, rescaling (enlarger) attack and sharpening attack. In addition, the proposed watermarking method using FOA can accelerate the finding of optimal scaling factor.

V. CONCLUSIONS

In this paper, a novel image watermarking method based on DWT-HD-SVD transforms is proposed. Specifically, the FOA is used to find the optimal scaling factor. The invisibility and robustness of this method are analyzed by the numerical simulation experiments and the results show the watermarked host images have good visual quality, PSNRs, and SSIMs. Besides, the watermarks can be clearly extracted from the watermarked host image under different attacks with the relatively high NCs. Moreover, even for the watermarks with different sizes, the proposed image watermarking method can achieve a good invisibility and robustness. In addition, the comparison with the related works are listed and the corresponding metric values show that the proposed method has a better performance in terms of robustness for most attacks. It is worth noting that the proposed method is highly robust to defend the filter, noise, JPEG compression, JPEG2000 compression and sharpening attack. In the future work, the proposed watermarking method may be need to pay attention on resisting more attack, such as rotation attack and cropping attack. In addition, the watermarking performance can be further improved if using enhanced FOA algorithm.

REFERENCES

- [1] I. J. Cox, J. Kilian, F. T. Leighton, and T. Shamoan, "Secure spread spectrum watermarking for multimedia," *IEEE Trans. Image Process.*, vol. 6, no. 12, pp. 1673–1687, Dec. 1997.
- [2] N. Nikolaidis and I. Pitas, "Robust image watermarking in the spatial domain," *Signal Process.*, vol. 66, no. 3, pp. 385–403, 1998.
- [3] J. Song, J. Song, and Y. Bao, "A blind digital watermark method based on SVD and chaos," in *Proc. Int. Workshop Inf. Electron. Eng.*, 2012, pp. 285–289.
- [4] X. Li, S.-T. Kim, and I.-K. Lee, "Robustness enhancement for image hiding algorithm in cellular automata domain," *Opt. Commun.*, vol. 356, no. 1, pp. 186–194, 2015.
- [5] Q. Su, Y. Niu, H. Zou, Y. Zhao, and T. Yao, "A blind double color image watermarking algorithm based on QR decomposition," *Multimedia Tools Appl.*, vol. 72, no. 1, pp. 987–1009, 2014.
- [6] S. D. Lin and C.-F. Chen, "A robust DCT-based watermarking for copyright protection," *IEEE Trans. Consum. Electron.*, vol. 46, no. 3, pp. 415–421, Aug. 2000.
- [7] M. Barni, F. Bartolini, V. Cappellini, and A. Piva, "A DCT-domain system for robust image watermarking," *Signal Process.*, vol. 66, no. 3, pp. 357–372, May 1998.
- [8] J. C. Patra, J. E. Phua, and C. Bornand, "A novel DCT domain CRT-based watermarking scheme for image authentication surviving JPEG compression," *Digit. Signal Process.*, vol. 20, no. 6, pp. 1597–1611, 2010.
- [9] F. Ernawan and M. N. Kabir, "A robust image watermarking technique with an optimal DCT-psychovisual threshold," *IEEE Access*, vol. 6, pp. 20464–20480, 2018.
- [10] A. K. Singh, B. Kumar, S. K. Singh, S. P. Ghrera, and A. Mohan, "Multiple watermarking technique for securing online social network contents using back propagation neural network," *Future Gener. Comput. Syst.*, vol. 86, no. 1, pp. 926–939, 2018.
- [11] A. K. Singh, "Improved hybrid algorithm for robust and imperceptible multiple watermarking using digital images," *Multimedia Tools Appl.*, vol. 76, no. 6, pp. 8881–8900, 2017.
- [12] T. K. Tsui, X.-P. Zhang, and D. Androutsos, "Color image watermarking using multidimensional Fourier transforms," *IEEE Trans. Inf. Forensic Security*, vol. 3, no. 1, pp. 16–28, Mar. 2008.
- [13] V. Solachidis and L. Pitas, "Circularly symmetric watermark embedding in 2-D DFT domain," *IEEE Trans. Image Process.*, vol. 10, no. 11, pp. 1741–1753, Nov. 2001.
- [14] P. Tao and A. M. Eskicioglu, "An adaptive method for image recovery in the DFT domain," *J. Multimedia*, vol. 1, no. 6, pp. 36–45, 2006.
- [15] Y. Wang, J. F. Doherty, and R. E. V. Dyck, "A wavelet-based watermarking algorithm for ownership verification of digital images," *IEEE Trans. Image Process.*, vol. 11, no. 2, pp. 77–88, Feb. 2002.
- [16] M.-S. Hsieh, D.-C. Tseng, and Y.-H. Huang, "Hiding digital watermarks using multiresolution wavelet transform," *IEEE Trans. Ind. Electron.*, vol. 48, no. 5, pp. 875–882, Oct. 2001.
- [17] Z. H. Wei, P. Qin, and Y. Q. Fu, "Perceptual digital watermark of images using wavelet transform," *IEEE Trans. Consum. Electron.*, vol. 44, no. 4, pp. 1267–1272, Nov. 1998.
- [18] Q. Su, Y. Niu, Y. Zhao, S. Pang, and X. Liu, "A dual color images watermarking scheme based on the optimized compensation of singular value decomposition," *AEU-Int. J. Electron. Commun.*, vol. 67, no. 8, pp. 652–664, 2013.
- [19] M.-Q. Fan, H.-X. Wang, and S.-K. Li, "Restudy on SVD-based watermarking scheme," *Appl. Math. Comput.*, vol. 203, no. 2, pp. 926–930, 2008.
- [20] K.-L. Chung, W.-N. Yang, Y.-H. Huang, S.-T. Wu, and Y.-C. Hsu, "On SVD-based watermarking algorithm," *Appl. Math. Comput.*, vol. 188, no. 1, pp. 54–57, 2007.
- [21] S. Thakur, A. Singh, and S. Ghrera, "NSCT domain-based secure multiple-watermarking technique through lightweight encryption for medical images," *Concurrency Comput., Pract. Exper.*, vol. 31, p. e5108, Dec. 2018.
- [22] N. Agarwal, A. K. Singh, and P. K. Singh, "Survey of robust and imperceptible watermarking," *Multimedia Tools Appl.*, vol. 78, no. 7, pp. 8603–8633, 2019.
- [23] N. Muhammad and N. Bibi, "Digital image watermarking using partial pivoting lower and upper triangular decomposition into the wavelet domain," *IET Image Process.*, vol. 9, no. 9, pp. 795–803, Sep. 2015.
- [24] X. Ye, X. Chen, M. Deng, and Y. Wang, "A SIFT-based DWT-SVD blind watermark method against geometrical attacks," in *Proc. 7th Int. Congr. Image Signal Process.*, Oct. 2014, pp. 323–329.
- [25] R. Mehta, N. Rajpal, and V. P. Vishwakarma, "LWT-QR decomposition based robust and efficient image watermarking scheme using Lagrangian SVR," *Multimedia Tools Appl.*, vol. 75, no. 7, pp. 4129–4150, 2016.
- [26] S. Murty and P. R. Kumar, "A robust digital image watermarking scheme using hybrid DWT-DCT-SVD technique," *J. Comput. Sci. Netw. Secur.*, vol. 10, no. 10, pp. 185–192, 2010.

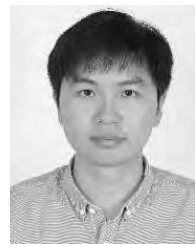
- [27] K. A. Navas, A. M. Cheriyan, M. Lekshmi, T. S. Archana, and M. Sasikumar, "DWT-DCT-SVD based watermarking," in *Proc. 3rd Int. Conf. Commun. Syst. Softw. Middleware Workshops*, Jan. 2007, pp. 271–274.
- [28] V. Santhi, N. Rekha, and S. Tharini, "A hybrid block based watermarking algorithm using DWT-DCT-SVD techniques for color images," in *Proc. Int. Conf. Comput., Commun. Netw.*, Dec. 2008, pp. 1–7.
- [29] N. H. Divecha and N. Jani, "Image watermarking algorithm using DCT, DWT and SVD," in *Proc. Nat. Conf. Innov. Paradigms Eng. Technol.*, 2012, pp. 13–16.
- [30] O. Jane and E. Elba i, "A new approach of nonblind watermarking methods based on DWT and SVD via LU decomposition," *Turkish J. Electr. Eng. Comput. Sci.*, vol. 22, no. 5, pp. 1354–1366, 2014.
- [31] Q. Su and B. Chen, "A novel blind color image watermarking using upper Hessenberg matrix," *AEU-Int. J. Electron. Commun.*, vol. 76, no. 6, pp. 64–71, 2017.
- [32] Q. Su, "Novel blind colour image watermarking technique using Hessenberg decomposition," *IET Image Process.*, vol. 10, no. 11, pp. 817–829, Nov. 2016.
- [33] J.-M. Guo, G.-H. Lai, K. Wong, and L.-C. Chang, "Progressive halftone watermarking using multilayer table lookup strategy," *IEEE Trans. Image Process.*, vol. 24, no. 7, pp. 2009–2024, Jul. 2015.
- [34] M. Ali, C. W. Ahn, and P. Siarry, "Differential evolution algorithm for the selection of optimal scaling factors in image watermarking," *Eng. Appl. Artif. Intell.*, vol. 31, no. 31, pp. 15–26, 2014.
- [35] I. A. Ansari, A. Pant, and C. W. Ahn, "Robust and false positive free watermarking in IWT domain using SVD and ABC," *Eng. Appl. Artif. Intell.*, vol. 49, pp. 114–125, Mar. 2016.
- [36] I. A. Ansari, M. Pant, and C. W. Ahn, "Artificial bee colony optimized robust-reversible image watermarking," *Multimedia Tools Appl.*, vol. 76, no. 17, pp. 18001–18025, 2017.
- [37] A. Mishra, C. Agarwal, A. Sharma, and P. Bedi, "Optimized gray-scale image watermarking using DWT-SVD and firefly algorithm," *Expert Syst. Appl.*, vol. 41, no. 17, pp. 7858–7867, 2014.
- [38] Y. Guo, B. Z. Li, and N. Goel, "Optimised blind image watermarking method based on firefly algorithm in DWT-QR transform domain," *IET Image Process.*, vol. 11, no. 6, pp. 406–415, Jun. 2017.
- [39] V. Aslantas, A. Dogan, and S. Ozturk, "DWT-SVD based image watermarking using particle swarm optimizer," in *Proc. IEEE Int. Conf. Multimedia Expo*, Apr./Jun. 2008, pp. 241–244.
- [40] W.-T. Pan, "A new fruit fly optimization algorithm: Taking the financial distress model as an example," *Knowl.-Based Syst.*, vol. 26, pp. 69–74, Feb. 2012.
- [41] Z. Xiao, J. Sun, Y. Wang, and Z. Jiang, "Wavelet domain digital watermarking method based on fruit fly optimization algorithm," *J. Comput. Appl.*, vol. 35, no. 9, pp. 2527–2530, 2015.
- [42] S. Luo, K. Sarabandi, L. Tong, and L. Pierce, "A LS-SVM-based classifier with fruit fly optimization algorithm for polarimetric SAR images," in *Proc. IEEE Int. Geosci. Remote Sens. Symp.*, Jul. 2016, pp. 1859–1862.
- [43] M. Yang, N.-B. Liu, and W. Liu, "Image 1D OMP sparse decomposition with modified fruit-fly optimization algorithm," *Cluster Comput.*, vol. 20, no. 4, pp. 3015–3022, 2017.
- [44] R. Hu, S. Wen, Z. Zeng, and T. Huang, "A short-term power load forecasting model based on the generalized regression neural network with decreasing step fruit fly optimization algorithm," *Neurocomputing*, vol. 221, pp. 24–31, Jan. 2017.
- [45] T. Li, L. Gao, P. Li, and Q. Pan, "An ensemble fruit fly optimization algorithm for solving range image registration to improve quality inspection of free-form surface parts," *Inf. Sci.*, vols. 367–368, pp. 953–974, Nov. 2016.
- [46] R.-S. Run, S.-J. Horng, J.-L. Lai, T.-W. Kao, and R.-J. Chen, "An improved SVD-based watermarking technique for copyright protection," *Expert Syst. Appl.*, vol. 39, no. 1, pp. 673–689, 2012.



JIADONG HUANG received the bachelor's degree in communication engineering from Shanghai Second Polytechnic University, China, in 2016. He is currently pursuing the master's degree with the School of Electronic Engineering, Guangxi Normal University. His research interests include image watermarking and image encryption.



YULING LUO received the Ph.D. degree in information and communication engineering from the South China University of Technology, Guangzhou, China. She is currently an Associate Professor with the School of Electronic Engineering, Guangxi Normal University, Guilin, China. Her research interests include information security, image processing, chaos theory, and embedded system implementations.



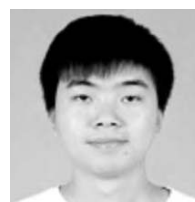
LVCHEN CAO received the B.Eng. degree in electronic and information engineering from the Zhongyuan University of Technology, Zhengzhou, China, in 2013, and the M.S. degree in electronic science and technology from Guangxi Normal University, Guilin, China, in 2016. He is currently pursuing the Ph.D. degree with the Beijing Institute of Technology. He was an Algorithm Engineer with ALi Corporation, Zhuhai, China, from 2016 to 2017. His current

research interests include pattern recognition, machine learning, and chaotic cryptography.



SU YANG received the B.A. degree in mechanical engineering from the Changchun University of Technology, Changchun, China, in 2008, the M.Sc. degree in information technology from the University of Abertay Dundee, Dundee, U.K., in 2010, and the Ph.D. degree in electronic engineering from the University of Kent, Canterbury, U.K., in 2015. During the Ph.D. degree, he was with the Intelligent Interactions Research Group, School of Engineering and Digital Arts, where his research was focusing on using EEG for biometric person recognition. He was with Temple University, Philadelphia, PA, USA, as a Postdoctoral Research Associate with the College of Engineering, from 2016 to 2017. He is currently a Senior Research Associate with the Intelligent Systems Research Centre, Ulster University, Londonderry, U.K. His current research interests include signal processing, pattern recognition, EEG-event detection, and MEG source reconstruction/localization.

DUQU WEI, photograph and biography not available at the time of publication.



RONGLONG ZHOU received the B.Eng. degree in electronics and information engineering from the Heilongjiang University of Finance and Economics, China, in 2015, and the M.Eng. degree from Guangxi Normal University, China, in 2018. His research interests include multimedia security and nonlinear dynamical systems.

...

JUNXIU LIU, photograph and biography not available at the time of publication.